The Effects of Sulfite or Nitrate on Turnover-Dependent Inhibition in the ATPase from *Halobacterium saccharovorum* Are Related to the Binding of the Second Metal Ion†

Brigitte Schobert

Department of Physiology and Biophysics, University of California, Irvine, California 92717

Received July 23, 1993; Revised Manuscript Received September 21, 1993®

ABSTRACT: The turnover-dependent inhibition of the *Halobacterium saccharovorum* ATPase is dependent on two parameters: pH and the concentration of the divalent cation present. At pH 6 and 1 mM Mn^{2+} the inhibition is small, but increases steeply with 6 mM Mn^{2+}. In contrast, at pH 8.5 the inhibition is more than 90% at 1 mM Mn^{2+}, and higher concentrations have little additional effect. A relationship between the occupation of a second metal ion binding site and turnover-dependent inhibition was postulated previously [Schobert, B. (1992) *J. Biol. Chem. 267*, 10252–10257]. The results lead to a model where this site (X^-) can alternatively bind protons (XH), depending on the pH and the free metal ion concentration. The pK_a of XH is estimated to be 9. The turnover-dependent inhibition is diminished by bisulfite, whereas sulfite is ineffective. The kinetics show that bisulfite and metal ion compete for the same site. In the proposed model, bisulfite binds via its negative charge to the site from which P_i was released and is arranged such as to interact with X^- via its protonated group ($X—HSO_3^-$). In this way, formation of the inhibited enzyme species XMe is prevented. Inhibitory anions like nitrate, which carry a permanent dipole as a common feature, show uncompetitive inhibition vs metal ions. The data are compatible with a model in which these inhibitors bind to the vacant P_i site and position their positive charges near XH. As a consequence, the pK_a of XH is decreased and X^- is stabilized, which in turn favors the formation of XMe. The downshift in pK_a was calculated to be 0.7 pH unit.

F_1-ATPases from mitochondria and chloroplasts show nonlinear kinetics of ATP hydrolysis. Typically, the reaction starts with a fast rate that decreases continuously within the first minutes of the assay until a steady-state rate of much lower magnitude is reached (Vasilyeva et al., 1982a; Drobinskaya et al., 1985; Zhou et al., 1988; Guerrero et al., 1990). Although P_i is readily released from the enzyme, ADP (the other hydrolysis product) tends to be retained by the active site, and thus a large fraction of the ATPase is temporarily blocked and cannot enter another catalytic cycle (Bar-Zvi & Shavit, 1982; Feldman & Boyer, 1985; Drobinskaya et al., 1985; Chernyak & Kozlov, 1986; Zhou et al., 1988; Du & Boyer, 1989). Recently, it was shown that a very similar phenomenon could be observed with an ATPase from the halophilic archae *Halobacterium saccharovorum* (Schobert, 1991). This ATPase has a subunit composition somewhat similar to that of F_1-ATPases, but the individual subunits have larger molecular masses (Stan-Lotter & Hochstein, 1989; Bonet & Schobert, 1992). It has been suggested that the archaebacterial ATPases are closely related to F_0F_1-ATPases with respect to their quaternary structure (Tiedge & Schäfer, 1988) and hydrolytic mechanism (Schobert, 1991).

In earlier investigations of ATP hydrolysis kinetics with the ATPase from *H. saccharovorum* (Schobert & Lanyi, 1989), three parameters were introduced to describe the nonlinear curves: the initial rate v_1, the final rate v_2, and the transition rate k. The ratio v_2/v_1 is the fraction of active enzyme in the equilibrium that develops during turnover-dependent inhibition (Schobert, 1992) and is independent of the ATPase concentration used in the assay (within the P_i measuring range; Schobert, 1992). It was shown that the magnitude of this inhibition depends on the assay conditions and that excess divalent metal ions are the primary cause for the observed nonlinearity. Two metal ion binding sites were postulated: the first for Me^I that complexes phosphate groups of ATP, and the second for Me^{II} with an as yet unknown position. Occupation of this second site, X, by a divalent metal ion was proposed as the cause for the slow release of ADP after the completion of the ATP hydrolysis cycle (Schobert, 1992). After several reaction cycles, a mixture of inactive (Me^I–ADP–Me^{II}-bound) and active (free) enzyme develops, and at steady-state conditions the rate v_2 is proportional to the fraction of enzyme with site X not occupied by a metal ion. The fraction of blocked enzyme is thus dependent on the free metal ion concentration in the assay, the K_d of site X, and on other parameters investigated in this report.

Sulfite is known to activate both F_1-ATPases (Mal'yan & Akulova, 1978; Vasilyeva et al., 1982b; Anton & Jagendorf, 1983; Du & Boyer, 1990) and archaebacterial ATPases from *Sulfolobus acidocaldarius* (Lübben & Schäfer, 1987; Konishi et al., 1987) and *H. saccharovorum* (Schobert, 1991). It was shown earlier that activation by sulfite corresponds to reduction of the turnover-dependent inhibition, whereas v_1 is not affected (Vasilyeva et al., 1982b; Schobert, 1991). Inhibitory anions like nitrate or azide do not change v_1 either, but instead increase the turnover-dependent inhibition (Vasilyeva et al., 1982b; Schobert, 1991). For these compounds, the terms "activation" and "inhibition" are used differently from their classical meanings, because the effects on enzymatic activity occur only *after* the completion of a hydrolytic reaction cycle. Nitrate is described as a typical inhibitor for vacuolar (Bowman & Bowman, 1986) and archaebacterial ATPases (Mukohata

† Supported by Grant DE-FGOER 13525 from the U.S. Department of Energy.

® Abstract published in *Advance ACS Abstracts*, November 1, 1993.

0006-2960/93/0432-13204$04.00/0

& Yoshida, 1987; Lübben & Schäfer, 1987), whereas azide is considered a typical inhibitor for F_1-ATPases (Vasilyeva et al., 1982b). In an earlier investigation of the *H. saccharovorum* ATPase, it was demonstrated that nitrate and azide act in a very similar fashion, and their differences are apparently due to different binding constants (Schobert, 1991).

Earlier experiments with the *H. saccharovorum* ATPase were carried out at pH 7 only, but suggested that investigations of turnover-dependent inhibition over a wide pH range would be of value. In this report, the properties of site X and the effect of activators and inhibitors on this site are investigated. The data are compatible with a model in which these compounds act by affecting the binding of Me^{II} to site X either unfavorably or favorably.

MATERIALS AND METHODS

ATPase Preparation. The growth of strain M6 of *Halobacterium saccharovorum*, membrane preparation, and enzyme purification are described elsewhere (Schobert & Lanyi, 1989).

ATPase Assay. The assay mixtures are described in the figure legends. The solutions were incubated at 30 °C, and the enzymatic reaction was started by the addition of ATPase (final protein concentration: 15–50 μg/mL, depending on the experiment). P_i production was determined according to Lanzetta et al. (1979) and as described earlier (Schobert & Lanyi, 1989). The production of 100 nmol of P_i/mL corresponds to an OD change of 1.0 at 650 nm. Kinetic analysis was on an IBM-AT-type computer using a Lotus spreadsheet program. The rates v_1 and v_2 were determined from the curves of phosphate production vs time by fitting the solution of the rate equation for the transition between the fully active enzyme and an equilibrium mixture containing active and inactive enzyme:

$$E(t) = (E_1 - E_2)\exp(-kt) + E_2 \quad (1)$$

where $E(t)$ is the concentration of active enzyme (i.e., the rate of ATP hydrolysis) at t, E_1 and E_2 are the initial and final concentrations of active enzyme (i.e., the initial and final rates of hydrolysis, v_1 and v_2, respectively), and k is the rate constant for reaching the equilibrium. Calculation of binding constants was with the equations explained in Results and used Lotus spreadsheet programs. The maximum inhibition that could be obtained at high pH or metal ion concentration was not 100%, but 98%. To correct for this residual activity, 0.02 was subtracted from v_2/v_1 in all of the data shown.

Materials. Prior to the assays, sulfite, selenite, nitrate, azide, and sulfamate were prepared as concentrated stock solutions in 3.5 M KCl and adjusted to the desired pH.

RESULTS

pH Dependency of ATP Hydrolysis Kinetics. Figure 1A shows the dependency of the initial rate on the pH in the assay. At pH 6, v_1 was very low, but increased approximately 20-fold near pH 8.5. Furthermore, the hydrolysis kinetics differed greatly at high and low pH (Figure 1B). In spite of the high initial rate at pH 8, more than 90% of the enzyme was inhibited after several minutes, whereas at pH 6 turnover-dependent inhibition was much less. In the course of these experiments, it became evident that the proper choice of the buffer system was important for the investigation of the pH dependency. CHES[1] and CAPS buffers should be avoided, because they affect the catalytic rate through their rather high metal ion complexing abilities (data not shown).

Effect of pH and Metal Ion Concentration on Turnover-Dependent Inhibition. The effect of pH was investigated, together with increasing concentrations of metal ion, and the result is demonstrated in the three-dimensional graph in Figure 2A. At pH 6 and 1 mM total Mn^{2+} concentration, the turnover-dependent inhibition was very low but increased considerably with rising Mn^{2+} concentrations (between 1 and 6 mM). At pH 8.5, however, extensive turnover-dependent inhibition occurred even with 1 mM Mn^{2+}, and the Mn^{2+} concentration used made little difference.

The above result led to the conclusion that the binding site for Me^{II} not only interacts with metal ions but can alternatively bind protons. At pH 6, this site X seems to be mainly protonated (XH), but at lower proton concentrations the species X^- prevails, which is able to interact with the metal ion. Such a postulated competition between protons and metal ions assumes that both species XH and X^- are present in significant amounts in the pH range 6–8.5. In order to determine the pK_a of site X, the following model was developed (model A/B):

$$K_I = [X^-][H^+]/[XH] \quad (2)$$

$$K_{II} = [X^-][Me]/[XMe] \quad (3)$$

where Me represents a divalent metal ion. It is assumed that only the enzyme species containing XMe is inhibited, whereas those that contain X^- and XH are not. In the following equation, v_1 represents the total fraction of enzyme and includes all of the species, even the fraction which becomes XMe under steady state conditions. v_2 is proportional only to the fraction of enzyme that remains active under steady-state conditions. The magnitude of the turnover-dependent inhibition can thus be expressed as

$$\frac{v_2}{v_1} = \frac{[X^-] + [XH]}{[X^-] + [XH] + [XMe]} \quad (4)$$

If eqs 2 and 3 are combined with eq 4,

$$\frac{v_2}{v_1} = \frac{1}{\{1 + [Me]K_I/K_{II}(K_I + [H^+])\}} \quad (5)$$

The metal ion concentration in the assay is not completely constant in the pH range investigated, but is dependent on the pK_a of ATP. [Me] was established by the equations that follow.

$$K_{ATP} = [ATP^{4-}][H^+]/[ATP^{3-}] \quad (6)$$

Only the pK_a for the dissociation of the fourth proton has to be considered for the free metal ion concentration. The other pK_a values are low and do not change the free metal ion concentration significantly in the pH range investigated:

$$K_I = [ATP^{4-}][Me]/[MeATP^{2-}] \quad (7)$$

$$[MeATP^{2-}] = [ATP^0] - [ATP^{4-}] - [ATP^{3-}] \quad (8)$$

$$[MeATP^{2-}] = [Me^0] - [Me] \quad (9)$$

where $[ATP^0]$ and $[Me^0]$ represent the total concentrations of ATP and metal ion added to the assay mixture, respectively. Equations 6–9 were combined, and the resulting quadratic equation (not shown) was used to calculate K_{ATP}. Earlier results (Schobert, 1992) provided the values for K_I and [Me] at pH 7. The established pK_{ATP} was 4.83, much lower than the value determined earlier at zero ionic strength (pK = 7.7;

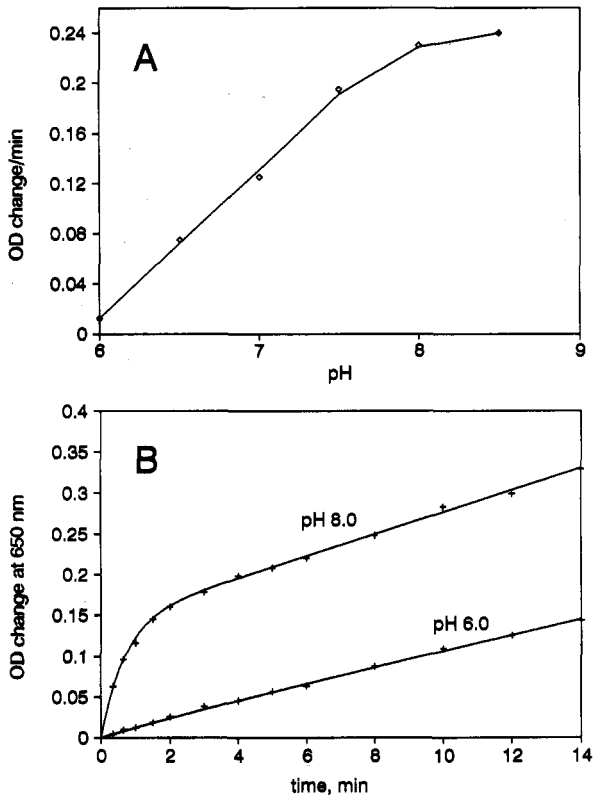

FIGURE 1: Effect of pH on ATP hydrolysis kinetics. (A) Dependence of v_1 on the pH of the assay solution. Each assay contained 3.5 M KCl, 2 mM $MnSO_4$, 10 mM ATP, ATPase (30 μg/mL), and 0.1 M of the following buffer systems: MES (at pH 6 and 6.5), MOPSO (at pH 7 and 7.5), EPPS (at pH 8), and AMPSO (at pH 8.5). (B) ATP hydrolysis kinetics at pH 6 and 8. Assay conditions were as described for A. The kinetic parameters were as follows: at pH 6, v_1 = 0.0125 OD/min, v_2 = 0.0097 OD/min, k = 0.3 min^{-1}; at pH 8, v_1 = 0.23 OD/min, v_2 = 0.0135 OD/min, k = 1.42 min^{-1}.

Smith & Martell, 1975). A downshift in this magnitude is not unexpected and is caused by the high salt concentration in the assay.

The quadratic equation was then solved for [Me] and resulted in

$$[Me] = -\{[ATP^0] - [Me^0] + K_1 + K_1[H^+]/K_{ATP}\}/2 + \{([ATP^0] - [Me^0] + K_1 + K_1[H^+]/K_{ATP})^2 - 4K_1[Me^0](-1 - [H^+]/K_{ATP})\}^{1/2}/2 \quad (10)$$

Equations 5 and 10 were combined and gave an equation with two unknowns: K_I and K_{II}. K_{II} was estimated previously in an earlier investation (formerly designated as K_2; Schobert, 1992), but these values are no longer applicable for model A/B. A competition with protons was not considered in the previous concept, and for this reason K_{II} can be expected to be much lower than its early version, K_2.

Model A/B was tested with a series of experiments similar to that shown in Figure 2A, using various metal ion concentrations and a wide pH range. If the model is correct, K_I and K_{II} will be constant at all pH values and metal ion concentrations used. The curves in Figure 2B were obtained by fitting them to the data points by trial and error, using those values for K_I and K_{II} which resulted in the best fit. Because the curves had to be fit with two unknowns that are related to each other, a series of pairs of K_I and K_{II} gave good fits to the

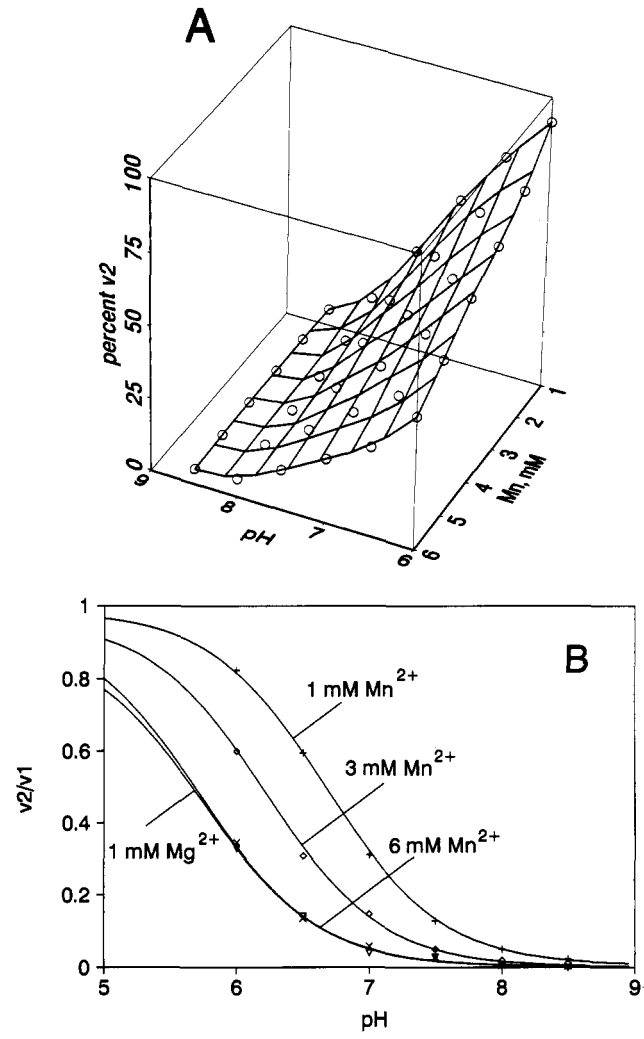

FIGURE 2: Dependence of turnover-dependent inhibition on pH and Mn^{2+} concentration. (A) Three-dimensional plot, created as a smoothed net over the entire range of values. The turnover-dependent inhibition is expressed as v_2 in percent of v_1. The assay solution contained 3.5 M KCl, 10 mM ATP, ATPase (30 μg/mL), the concentrations of $MnSO_4$ indicated on the z-axis, and a mixture of MES, MOPSO, EPPS, and AMPSO (0.1 M each), adjusted to the respective pH values indicated on the x-axis. (B) All curves were created with the best fit to the data points using model A/B (pK_I = 9, and K_{II} = 0.2 μM). The conditions were as described for A, with the the following Mn^{2+} concentrations (mM): (+) 1; (◇) 3; (×) 6; and (▽) 1 mM Mg^{2+}.

Table I: Constants for Models A/B, C, and D, Established as the Best Fits to the Data Shown in Figures 2B, 4A,B, and 6A–C

derived constants		equilibria
pK_I	9.0	$XH \leftrightarrow X^- + H^+$
pK_{IV}	5.9 (sulfite)	$HSO_3^- \leftrightarrow SO_3^{2-} + H^+$
	7.3 (selenite)	$HSeO_3^- \leftrightarrow SeO_3^{2-} + H^+$
pK_V	8.35 (nitrate)	$I^*XH \leftrightarrow I^*X^- + H^+$
	8.3 (azide)	
	8.3 (sulfamate)	
K_{II}	2×10^{-7} M	$XMe \leftrightarrow X^- + Me$
K_{III}	5×10^{-6} M (sulfite)	$XHA \leftrightarrow X^- + HA$
	5×10^{-5} M (selenite)	
K_{VI}	10^{-4} M (nitrate)	$I^*XH \leftrightarrow I + XH$
	6×10^{-3} M (azide)	
	10^{-1} M (sulfamate)	

[1] Abbreviations: AMPSO, 3-[(1,1-dimethyl-2-hydroxyethyl)amino]-2-hydroxypropanesulfonic acid; CAPS, 3-(cyclohexylamino)-1-propanesulfonic acid; CHES, 2-(*N*-cyclohexylamino)ethanesulfonic acid; EPPS, *N*-(2-hydroxyethyl)piperazine-*N*'-3-propanesulfonic acid; MES, 2-(*N*-morpholino)ethanesulfonic acid; MOPSO, 3-(*N*-morpholino)-2-hydroxypropanesulfonic acid.

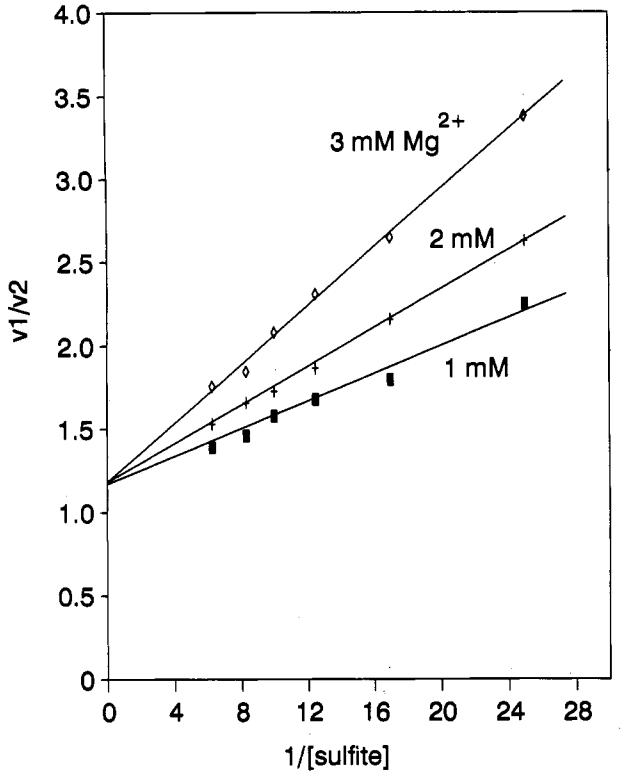

FIGURE 3: Double-reciprocal plot of v_2/v_1 vs sulfite concentration (M) in the presence of various Mg^{2+} concentrations. The assay mixture contained 3.5 M KCl, 10 mM ATP, 0.1 M MOPSO (pH 7), ATPase (30 μg/mL), the indicated concentrations of Na_2SO_3, and the following $MgSO_4$ concentrations (mM): (■) 1; (+) 2; (◇) 3.

data. Unique values for K_I and K_{II} were obtained by introducing another variable, i.e., Mn^{2+} concentration. For each Mn^{2+} concentration used, the calculated K_I and K_{II} values were plotted against each other. Three somewhat different curves resulted which intersected at one point (data not shown). The K_I and K_{II} values that describe this common point were used in calculating the lines in Figure 2B. They are listed in Table I. It is obvious from Figure 2B that the curves obtained are the titration curves of a group (XH), and the effect of increasing the metal ion concentration is phenomenologically identical to lowering the pK_a of this group. Mg^{2+} at 1 mM had an effect which is very similar to that at the highest Mn^{2+} concentration used. This result is in agreement with earlier findings (Schobert, 1992) which demonstrated that the dissociation constant of ATP and Mg^{2+} is much higher than that of ATP and Mn^{2+}. Because of this difference, the free Mg^{2+} concentration is always much higher than the free Mn^{2+} concentration under otherwise identical conditions.

Anions That Activate ATP Hydrolysis Compete with Metal Ions and Protons. An earlier study (Schobert, 1991) indicated that sulfite diminished the effect of excess metal ion and led to an investigation of the activating effect in the presence of increasing concentrations of metal ion. Mg^{2+} had to be used for these experiments, because of the limited solubility of $MnSO_3$ in 3.5 M KCl. The double-reciprocal plot in Figure 3 indicates competition between sulfite and Mg^{2+} for a site on the emzyme. This site is most likely X^-, but on the other hand an anionic site cannot bind an anionic group. However, if HSO_3^- is the effective species rather than SO_3^{2-}, interaction with the anionic X^- becomes feasible. If this prediction is valid, the activating effect should be proportional to the concentration of HSO_3^- at any given pH. The first pK_a of sulfurous acid is very low, but the second pK_a is 7.3 at low ionic strength (Perrin, 1982), although it will be somewhat lower at high salt concentrations. Therefore, in the pH range under investigation, a variable fraction of the anion will exist as the HSO_3^- species. Model C was developed to test this idea and to extend model A/B.

In addition to eqs 2 and 3, the following equations were included:

$$K_{III} = [X^-][HA]/[XHA] \quad (11)$$

$$K_{IV} = [H^+][A^-]/[HA] \quad (12)$$

where HA represents a weak acid like HSO_3^-, with the first proton lost but the second proton retained. It is assumed that XH is kinetically indistinguishable from X—HA and that turnover-dependent inhibition is absent when the binding site is in either state. Furthermore, HSO_3^- most likely also binds to a positively charged site on the protein. According to the model, this interaction does not affect the hydrolysis kinetics. K_{III} represents the overall affinity of the enzyme for this anion, which results from its proposed interaction with both the negative and positive groups. In analogy to eq 4, the steady-state rate relative to the initial rate is now proportional to the following species:

$$\frac{v_2}{v_1} = \frac{[X^-] + [XH] + [XHA]}{[X^-] + [XH] + [XHA] + [XMe]} \quad (13)$$

If eqs 2, 3, and 11 are combined with eq 13, model C is represented by the following equation:

$$\frac{v_2}{v_1} = \frac{\{1 + [H^+]/K_I + [HA]/K_{III}\}}{\{1 + [H^+]/K_I + [HA]/K_{III} + [Me]/K_{II}\}} \quad (14)$$

Equation 10 was applied for [Me], and [HA] was calculated from

$$[HA] = \frac{[HA^0]}{\{K_{IV}/[H^+] + 1\}} \quad (15)$$

where $[HA^0]$ represents the total concentration of the anion in the assay.

Model C was tested with several concentrations of sulfite in the pH range 6–8.5. Values for K_I and K_{II} were taken from the previous experiment (Table I), and K_{III} and K_{IV} had to be established by fitting the curves to the data points. The published ionization constant for sulfurous acid (Perrin, 1982) could not be applied, because of the high salt concentration in the assay. K_{III} and pK_{IV} at different sulfite concentrations were established as described for Figure 2B (see Table I). It is shown in Figure 4A that sulfite activates dramatically in the middle pH region (between pH 6 and 7), but its effect decreases steeply with rising pH. The affinity for sulfite is rather high, but its pK_a is considerably reduced in high salt (5.9 instead of 7.3; Table I). The results are consistent with the concept of model C in which binding of the metal ion to X^- is diminished by the interaction of X^- and HSO_3^-. The concentration of species HSO_3^-, however, decreases with increasing pH in accordance with the dissociation constant for this proton. From this point of view, it was interesting to investigate the effect of a compound similar to sulfite, but with a different pK_a for the second proton. Selenite (pK_a = 8.3; Perrin, 1982) was described earlier as an activating anion for F_1-ATPases (Carmeli et al., 1986) and was chosen for the following experiment. Because of solubility problems, only low concentrations of selenite could be employed. The curves in Figure 4B are plotted as in Figure 4A and show the expected

difference. Because the pK_a of selenite is approximately 1 pH unit higher than that of sulfite, the curves have different shapes and do not drop off as steeply toward higher pH values. To demonstrate this effect of selenite more clearly, a curve was created for 200 mM selenite using the same constants as for the other two curves with selenite. It should be emphasized that because of solubility problems this curve could not be verified experimentally (Figure 4B). The activating effect of selenite was less dramatic than was expected from its high pK_a. The reason is a much lower affinity of the ATPase for selenite than for sulfite (Table I).

Anions That Inhibit ATP Hydrolysis Lower the pK_a of Site X. An earlier study (Schobert, 1991) established that nitrate was not only able to increase the turnover-dependent inhibition but also antagonized the effect of sulfite, i.e., the effects of these anions were related to one another. The relationship between site X and nitrate was tested with a series of metal ion and nitrate concentrations, similar to the above studies of sulfite. The double-reciprocal plot in Figure 5 indicates that the interaction between nitrate and metal is kinetically uncompetitive, and thus binding of nitrate to site X is not expected. However, the presence of nitrate in the environment of site X appears to increase its apparent metal ion binding affinity. These results and considerations led to model D, which is another extension of model A/B. In addition to eqs 2 and 3, the following equations were included:

$$K_V = [I^*X^-][H^+]/[I^*XH] \quad (16)$$

$$K_{VI} = [XH][I]/[I^*XH] \quad (17)$$

$$K_{VII} = [I^*X^-][Me]/[I^*XMe] \quad (18)$$

where I* represents an inhibitor bound to a site on the enzyme that is different from X. The enzyme concentration is in the nanomolar range, and binding of an inhibitor, added in millimolar concentrations, does not change the total concentration, $[I^0]$, significantly; therefore, [I] can be considered equal to $[I^0]$. In analogy to eq 4, the steady-state rate relative to the initial rate is proportional to the concentrations of the following enzyme species:

$$\frac{v_2}{v_1} = \frac{[X^-] + [XH] + [I^*X^-][I^*XH]}{[X^-] + [XH] + [XMe] + [I^*X^-] + [I^*XH] + [I^*XMe]} \quad (19)$$

Equations 2, 3, and 16–18 were combined to solve eq 19, which resulted in

$$\frac{v_2}{v_1} = [(1 + [H^+]/K_I + [I]/K_{VI} + [I][H^+]/K_{VI}K_V)]/[(1 + [H^+]/K_I + [Me]/K_{II} + [I]/K_{VI} + [I][H^+]/K_{VI}K_V + [I][Me]/K_{VII}K_{VI})] \quad (20)$$

Equation 10 was employed for [Me]. Model D was tested in a manner similar to the previous models over the pH range 6–8.5 and with different inhibitor concentrations. K_V and K_{VI} were established as described for Figure 2B. K_I and K_{II} were taken from the previous experiment (Table I). It was assumed that the binding of the inhibitor does not change the affinity for Me^{II}, and therefore $K_{VII} = K_{II}$. The data in Figure 6A indicate that pK_V is lower than pK_I (Table I). As expected, binding of nitrate induces a downshift in the pK_a of site X of approximately 0.7 pH unit. Addition of nitrate and an increase in free metal ion concentration yield phenomenologically the same result (compare Figure 2B). A similar result was obtained with azide (Figure 6B), except that the affinity of the enzyme toward the inhibitor was lower, and higher concentrations had to be employed for a comparable effect (Table I). As a third example, another anion was found which inhibits the ATPase in the same fashion as nitrate and azide. Figure 6C shows the effect of sulfamate on turnover-dependent inhibition. It is noteworthy that this compound carries a SO_3 group, like sulfite, and yet has the opposite, i.e., inhibitory, effect. The affinity for this anion was very low, but the pK_a shift was of equal magnitude (Table I).

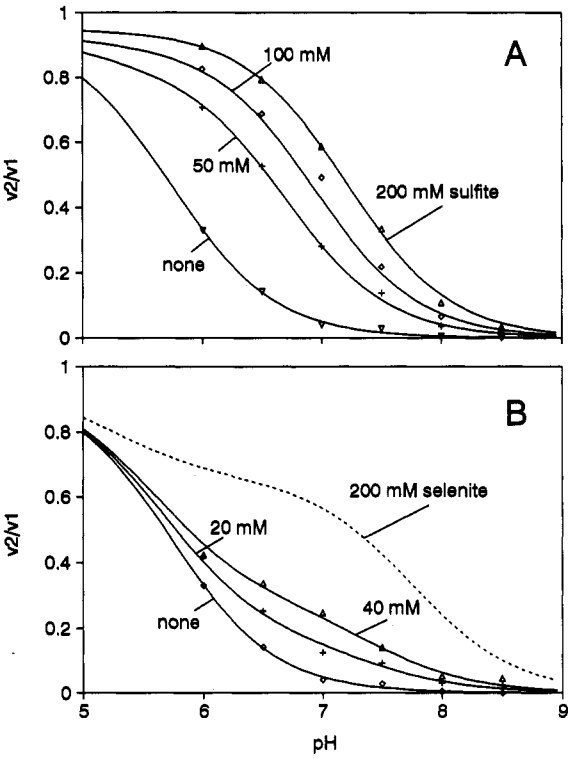

FIGURE 4: Dependence of turnover-dependent inhibition on pH and activator concentration. (A) The effect of sulfite; all curves were created with the best fit to the data points using model C (pK_{IV} = 5.9, K_{III} = 5 μM) and the constants established before (Figure 2B). The assay mixture contained 3.5 M KCl, 10 mM ATP, 1 mM $MgSO_4$, 0.1 M buffer (as described for Figure 1A), ATPase (30 μg/mL), and the following concentrations of sulfite (mM): (▽) 0; (+) 50; (◇) 100; (△) 200. (B) The effect of selenite; all curves were created as described for A, but with pK_{IV} = 7.3 and K_{III} = 50 μM. The assay mixture was as described for A, but with the following selenite concentrations (mM): (◇) 0; (+) 20; (△) 40. The dashed curve was simulated for 200 mM selenite, but could not be obtained experimentally.

DISCUSSION

The turnover-dependent inhibition of F_1-ATPases has been known for many years [Boyer (1993) and references therein], but it is still not fully understood. Boyer (1993) came to the conclusion that the Mg^{2+}- and ADP-inhibited enzyme probably is not an intermediate in the course of hydrolysis, but represents a less active species. An inhibitory effect of divalent cations, especially Mg^{2+}, was reported earlier (Hochman et al., 1976; Anthon & Jagendorf, 1983; Hochman & Carmeli, 1981; Guerrero et al., 1990; Murataliev, 1992). However, in these investigations the anomalous kinetics was either not considered at all (Hochman & Carmeli, 1981; Anthon & Jagendorf, 1983), both initial and steady-state rates were shown to be

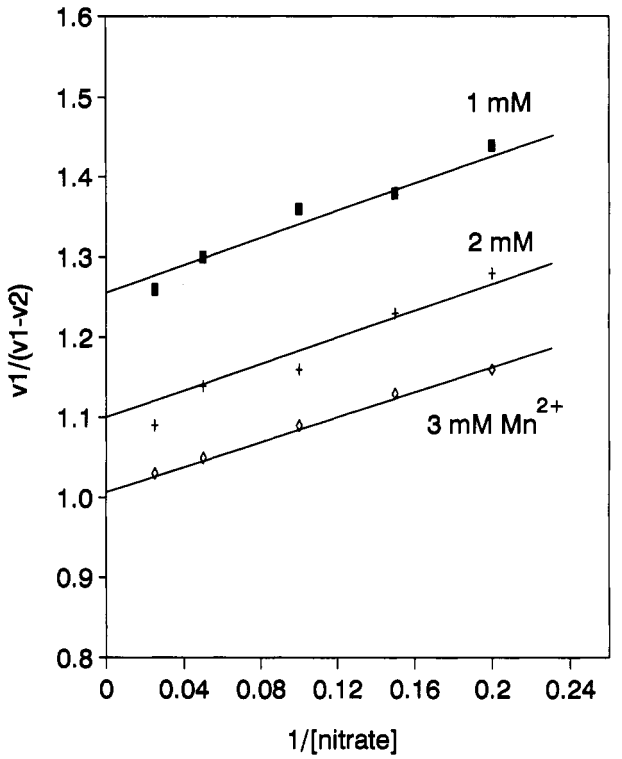

FIGURE 5: Double-reciprocal plot of $(v_1 - v_2)/v_1$ vs nitrate concentration (mM) in the presence of various Mn^{2+} concentrations. The assay mixture contained 3.5 M KCl, 10 mM ATP, 0.1 M MES (pH 6.5), ATPase (50 μg/mL), the indicated concentrations of $NaNO_3$, and the following $MnSO_4$ concentrations (mM): (■) 1; (+) 2; (◇) 3.

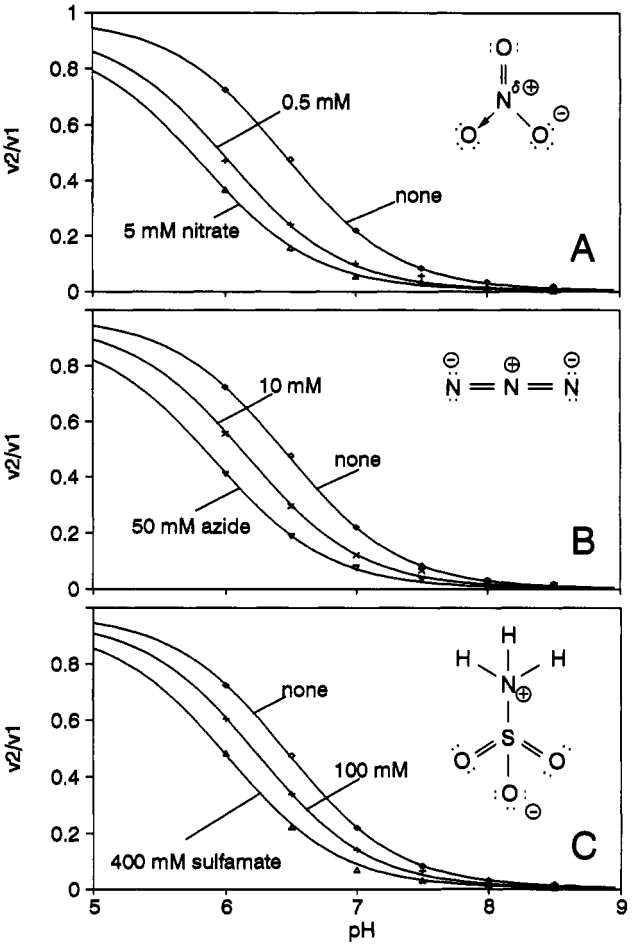

FIGURE 6: Dependence of turnover-dependent inhibition on pH and inhibitor concentration and structures of nitrate, azide, and sulfamate. (A) The effect of nitrate; all curves were created with the best fit to the data points using model D ($pK_V = 8.35$, $K_{VI} = 0.1$ mM) and the constants established before (Figure 2B). The assay mixture contained 3.5 M KCl, 10 mM ATP, 2 mM $MnSO_4$, 0.1 M buffer (as described for Figure 1A), ATPase (50 μg/mL), and the following concentrations of nitrate (mM): (◇) 0; (+) 0.5; (△) 5. (B) The effect of azide; all curves were created with the best fit to the data points using model D ($pK_V = 8.3$, $K_{VI} = 6$ mM) and the constants established before (Figure 2B). The assay mixture was as described for A, but with the following azide concentrations (mM): (×) 10; (▽) 50. (C) The effect of sulfamate; all curves were created with the best fit to the data points using model D ($pK_V = 8.3$, $K_{VI} = 0.1$ M) and the constants established before (Figure 2B). The assay mixture was as described before, but with the following sulfamate concentrations (mM): (+) 100; (△) 400.

inhibited by Mg^{2+} (Guerrero et al., 1990), or tight binding of inhibitory ADP was believed to precede Mg^{2+} binding (Murataliev, 1992) rather than to be caused by Mg^{2+} binding. Some of the latter results were obtained in the presence of azide (Murataliev, 1992), which made it difficult to resolve the individual effects. Mal'yan and Akulova (1978) described the pH dependence of the sulfite effect and recognized the importance of the pK_a's of activators. However, they did not take into consideration the biphasic kinetics and thus could not explain the observed effects. Anthon and Jagendorf (1983) concluded that the inhibitory Mg^{2+} binds to a site different from the MgATP binding site and that, in the presence of sulfite, the K_i for Mg^{2+} is raised. Vasilyeva et al. (1982b) came to the conclusion that sulfite or azide acts by increasing or decreasing the fraction of inactive enzyme containing tightly bound ADP. Du and Boyer (1990) had a similar explanation. A connection with metal ion binding, however, was not reported by these groups.

This work with the *H. saccarovorum* ATPase makes a connection between the effects of excess metal ion, established earlier (Schobert, 1992), and the influence of pH and various anionic activators and inhibitors. A search for compounds that activate the *H. saccharovorum* enzyme indicated that an activator needs to fulfill certain requirements (data not shown). It has to carry at least two acidic groups with very different pK_a's. The pK_a of the first group should be low (near 1), while the pK_a of the second group has to be at least 5.5. Cationic acids with similar pK_a values are ineffective, as found earlier also by Mal'yan and Akulova (1978). Furthermore, the anion has to be small.

Relatively few compounds fulfill these requirements, but bicarbonate, phosphate, pyrophosphate, and arsenate belong to this category. Bicarbonate activates both MF_1 (Nelson et al., 1972) and CF_1 (Hochman & Carmeli, 1981; Guerrero et al., 1990) and the *H. saccharovorum* ATPase (not shown). However, experiments with this compound could not be conducted at a pH lower than 7.5. Another problem arose with phosphate. It was shown earlier with the coupled assay system (using pyruvate kinase and lactate dehydrogenase to monitor ATPase activity) that phosphate does, in principle, activate (Schobert, 1991). However, control experiments indicated that the indirect assay system does not agree with the direct assay over the entire range of pH's and metal ion concentrations used. Furthermore, phosphate or pyrophosphate shows limited solubility at high salt. Because of these difficulties, they could not be included in the present investigation.

Activation by phosphate or arsenate was shown earlier for CF_1 (Carmeli & Lifshitz, 1972) and by pyrophosphate for MF_1 (Kalashnikova et al., 1988). The latter group concluded that the activation is caused by the binding of pyrophosphate to noncatalytic sites. Earlier, monobasic carboxylic acids were

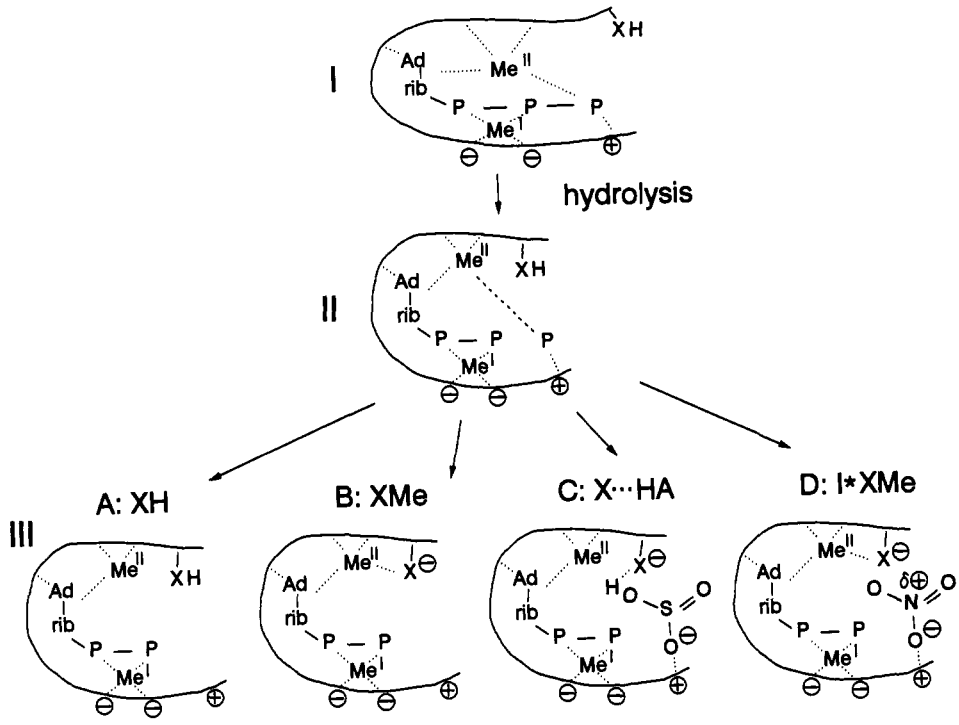

FIGURE 7: Model of the arrangements of ATP or ADP, the two metal ions, and site X at the catalytic site of the ATPase. For convenience, only one catalytic site is shown in the scheme. State I represents the binding of ATP and the metal ions before hydrolysis. State II represents the state immediately after hydrolysis, but with P_i not yet released. State III illustrates the different forms of X and the interaction of activator or inhibitor molecules with the binding of ADP–Me^I–Me^{II}. See text for further explanation.

reported to exert an activating effect also (Mal'yan & Akulova, 1978). This result was confirmed with the *H. saccharovorum* ATPase (not shown). However, these compounds act by a different principle: they reduce the concentration of free divalent metal ions by the formation of complexes. The criterion for such an effect is not only the reduction of turnover-dependent inhibition but also the decrease in v_1 in response to rising activator concentrations (Schobert, 1992). Some of the acids listed above (bicarbonate, phosphate) possess complexing abilities also and, thus, function according to both principles.

What distinguishes nitrate, azide, and sulfamate from the anionic activators, and which properties do they have in common to account for their effects on the enzyme kinetics? Unlike the activators they have only one protonatable group, and because they are strong acids, they cannot exist as protonated species in the pH range 6–8.5. However, in addition to their negative charge, these molecules carry a full or partial positive charge. Nitrate contains three different types of bonding between the N and O atoms: a σ–π double-bond, a σ single bond, and a coordinate bond for which the nitrogen provides both electrons. This is the main cause for the overall dipole moment in nitrate (2.17 D in HNO_3; Dean, 1985). Azide carries a partial positive charge in all three resonance structures (0.8 D in HN_3; Dean, 1985), and sulfamate exists as a zwitterion in the pH region under investigation (Burton & Nickless, 1968). If the negative moiety of the inhibitor binds to a positive group on the protein, which is near site X, the positive charge on the inhibitor molecule could be positioned in the immediate vicinity of X. Such a change in the charge distribution will lower the pK_a of XH. The reason for the different effectiveness of the three inhibitors may be in their geometry. Nitrate is a trigonal planar molecule and appears to fit best into the active site of the *H. saccharovorum* ATPase, whereas azide is a rod-shaped molecule and is not as well stabilized by groups provided by the enzyme. Sulfamate is a longer and bulkier molecule and will fit into the site with a lower probability. Supporting groups in the active site of F_1-ATPases are probably not in the same position as in archaebacterial ATPases, and this explains their different inhibitor specificities.

The results in this article support the models illustrated schematically in Figure 7. In state I, Me^{II} is coordinated to the third phosphate group, most likely to the nucleotide and to two other groups of as yet unidentified nature. Site X is so far removed from Me^{II} that an interaction is not feasible. After the cleavage of ATP, a conformational change takes place and site X is positioned close to Me^{II}, whereas P_i is removed from the metal ion (state II). P_i is released in the following step and leads to the formation of different enzyme species, depending on the conditions (state III). X is protonated at low pH and thus is unable to replace the removed phosphate ligand of Me^{II}. As a result, a complex between enzyme and Me^I–ADP–Me^{II} is formed in which probably H_2O (not shown) is now the fourth ligand (state IIIA). Complexes between metal ions and ligands of very different nature are often unstable, and Me^I–ADP–Me^{II} is released as the consequence. After conformational recovery, a new cycle can begin with state I. If site X exists mainly as X^- (at high pH), it can function as an alternate ligand to Me^{II}. The resulting complex is energetically favored, because the ligands have the right properties and distances to Me^{II} (state IIIB). Bisulfite or similar activators formally convert group X^- into the protonated species (state IIIC). Bisulfite binds via its negatively charged group to a site which is as yet unkown, but might very well be the vacant P_i binding site. Such a binding location was already proposed by Du and Boyer (1990). Binding of bisulfite to this site would also explain why the activator is unable to interfere with v_1. The situation in IIIC is very similar to that in IIIA and leads to the fast release of ADP. The affinity for the activator is then decreased as a result of a conformational recovery, and bisulfite is released

as well. State IIID illustrates that nitrate can also interact with the vacant P_i binding site and bring its partial positive charge close to site X. With this arrangement species X^- is stabilized and ligand formation with Me^{II} is favored, as in state IIIB. This model also supports earlier observations (Schobert, 1991) which showed that sulfite and nitrate diminish each others' effect when present together in the assay.

Striking similarities exist between the *H. saccharovorum* ATPases and F_1-ATPases in almost all of the reactions shown and indicate that the proposed principles and reactions (Figure 7) are also applicable for the latter group. Although the models are not proven at this stage, they indicate that an understanding of turnover-dependent inhibition is an important aspect of the exploration of the ATPase mechanism.

ACKNOWLEDGMENT

I thank Dr. J. K. Lanyi for support and many stimulating discussions.

REFERENCES

Anthon, G. E., & Jagendorf, A. T. (1983) *Biochim. Biophys. Acta 723*, 358–365.
Bar-Zvi, D., & Shavit, N. (1982) *Biochim. Biophys. Acta 681*, 451–458.
Bonet, M. L., & Schobert, B. (1992) *Eur. J. Biochem. 207*, 369–376.
Bowman, B. J., & Bowman, E. J. (1986) *J. Membr. Biol. 94*, 83–97.
Boyer, P. D. (1993) *Biochim. Biophys. Acta 1140*, 215–250.
Burton, K. W. C., & Nickless, G. (1968) in *Inorganic Sulphur Chemistry* (Nickless, G., Ed.) p 618, Elsevier, Amsterdam.
Carmeli, C., & Lifshitz, Y. (1972) *Biochim. Biophys. Acta 267*, 86–95.
Carmeli, C., Huang, J. Y., Mills, D. M., Jagendorf, A. T., & Lewis, A. (1986) *J. Biol. Chem. 261*, 16969–16975.
Chernyak, B. V., & Kozlov, I. A. (1986) *Trends Biol. Sci. 11*, 32–35.
Dean, J. A., Ed. (1985) *Lange's Handbook of Chemistry*, p 101, McGraw-Hill, New York.
Drobinskaya, I. Y., Kozlov, I. A., Murataliev, M. B., & Vulfson, E. N. (1985) *FEBS Lett. 182*, 419–424.
Du, Z., & Boyer, P. D. (1989) *Biochemistry 28*, 873–879.
Du, Z., & Boyer, P. D. (1990) *Biochemistry 29*, 402–407.
Feldman, R. I., & Boyer, P. D. (1985) *J. Biol. Chem. 260*, 13088–13094.
Guerrero, K. J., Xue, Z., & Boyer, P. D. (1990) *J. Biol. Chem. 265*, 16280–16287.
Hochman, Y., & Carmeli, C. (1981) *Biochemistry 20*, 6287–6292.
Hochman, Y., Lanir, A., & Carmeli, C. (1976) *FEBS Lett. 61*, 255–259.
Kalashnikova, T. Y., Milgrom, Y. M., & Murataliev, M. B. (1988) *Eur. J. Biochem. 177*, 213–218.
Konishi, J., Wakagi, T., Oshima, T., & Yoshida, M. (1987) *J. Biochem. (Tokyo) 102*, 1379–1387.
Lanzetta, P. A., Alvarez, L. J., Reinach, P. S., & Candia, O. A. (1979) *Anal. Biochem. 100*, 95–97.
Lübben, M., & Schäfer, G. (1987) *Eur. J. Biochem. 164*, 533–540.
Mal'yan, A. N., & Akulova, E. A. (1978) *Biokhimiya 43*, 952–955.
Mukohata, Y., & Yoshida, M. (1987) *J. Biochem. (Tokyo) 101*, 311–318.
Murataliev, M. B. (1992) *Biochemistry 31*, 12885–12892.
Nelson, N., Nelson, H., & Racker, E. (1972) *J. Biol. Chem. 247*, 7657–7662.
Perrin, D. D. (1982) *Ionisation constants of inorganic acids and bases in aqueous solution*, Pergamon Press, New York.
Schobert, B. (1991) *J. Biol. Chem. 266*, 8008–8014.
Schobert, B. (1992) *J. Biol. Chem. 267*, 10252–10257.
Schobert, B., & Lanyi, J. K. (1989) *J. Biol. Chem. 264*, 12805–12812.
Smith, R. M., & Martell, A. E. *(1975) Critical stability constants*, Vol. 2, p 283, Plenum, New York.
Stan-Lotter, H., & Hochstein, L. I. (1989) *Eur. J. Biochem. 179*, 155–160.
Tiedge, H., & Schäfer, G. (1989) *Biochim. Biophys. Acta 977*, 1–9.
Vasilyeva, E. A., Minkov, I. B., Fitin, A. F., & Vinogradov, A. D. (1982a) *Biochem. J. 202*, 9–14.
Vasilyeva, E. A., Minkov, I. B., Fitin, A. F., & Vinogradov, A. D. (1982b) *Biochem. J. 202*, 15–23.
Zhou, J. M., Xue, Z., Du, Z., Melese, T., & Boyer, P. D. (1988) *Biochemistry 27*, 5129–5135.